第32卷 第9期　　焊　接　学　报　　Vol. 32　No. 9
2011年9月　TRANSACTIONS OF THE CHINA WELDING INSTITUTION　September 2011

脉冲电源双熔敷极焊条电弧焊焊缝熔深

菅明健，　邹增大，　王育福
（山东大学 材料液固结构演变与加工教育部重点实验室，济南　250061）


菅明健

摘　要：脉冲电源应用于双熔敷极焊条电弧焊，采用正交试验研究分析脉冲参数对焊缝熔深的影响. 结果表明，脉冲参数的变化引起焊缝熔深的相应变化，脉冲参数对焊缝熔深的影响程度由大到小的次序为峰值电流、频率、占空比、基值电流. 在试验范围内获得较大熔深时的脉冲参数分别是峰值电流为230～240 A，频率为3.3～3.7 Hz，占空比为48%～52%，基值电流为160～175 A. 脉冲频率为3.5 Hz、峰值电流230 A、基值电流160 A、占空比50%是获得较大熔深的脉冲参数优化组合. 脉冲电源应用于双熔敷极焊条电弧焊利于增加焊缝熔深.

关键词：脉冲参数；正交试验；熔深
中图分类号：TG444　　文献标识码：A　　文章编号：0253－360X(2011)09－0089－04

0　序　　言

焊缝的熔深、熔宽和余高是焊缝的主要几何参数，直接影响到焊缝质量. 对接接头焊缝最重要的尺寸是熔深，它直接影响到焊缝的承载能力[1]. 焊接工作者已对多种焊接工艺及参数对熔深的影响做了研究[2-5]. 双熔敷极焊条电弧焊(twin deposition electrode arc welding，TDEAW)作为一种新型的焊接工艺，在焊接领域有广泛的应用前景[6]. 这种焊接工艺工件不接电源，相比传统焊条电弧焊，焊缝熔深相对较浅. 研究脉冲电源应用于TDEAW对于焊缝熔深的影响规律，并在此基础上得出了试验范围内获得较大熔深时的脉冲参数，对于推广应用TDEAW具有重要意义.

1　双熔敷极焊条电弧焊

双熔敷极焊条电弧焊工件不接电源，焊条内两根平行且绝缘的焊芯分别接电源的两极，特制焊钳夹持焊条尾部，电弧形成于两根焊芯的端部之间，主要利用熔滴携带热量和弧柱热量熔化母材[7]，双熔敷极焊条电弧焊及焊条截面如图1所示. 熔敷极焊条电弧焊改变了被焊工件的焊接热循环，具有熔敷效率高、节约电能、工件上不存在活性斑点区、熔合比可调范围广等特点. 此焊接工艺相比传统焊条电弧焊，对工件的热输入相对较少，使得母材熔化量少，从而直接影响到焊缝与母材的熔合和焊缝的承载能力.

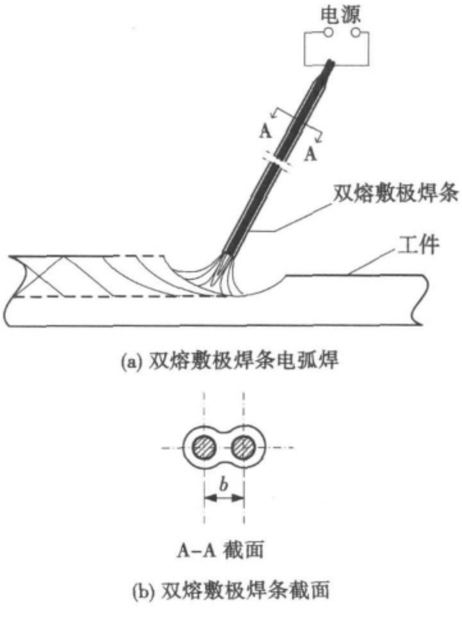

图1　双熔敷极焊条电弧焊及焊条截面示意图
Fig. 1　Diagrammatic sketch of twin deposition electrode arc welding and section of electrode

2　试验方法

试验用焊接电源是WSM-400逆变式脉冲氩弧焊机，其焊接脉冲参数有峰值电流、基值电流、频率

收稿日期：2010－07－19
基金项目：山东省自然科学基金资助项目(Z2006FF07)

和占空比，焊前或焊接过程中可以准确地设定，焊接过程中设置的参数恒定. 焊接过程中脉冲参数用 Agilent54624A 型示波器测定. 试验用焊条为自制涂压机压制的酸性双熔敷极焊条，焊芯为 H08A，尺寸为 ϕ4 mm × 400 mm，经 150 ℃ × 1 h 烘干. 药皮重量系数为 45.6%. 由于双熔敷极焊条两芯间距是控制电弧电压的最重要因素，试验中两芯间距为 5.4 mm (两焊芯之间的间隙为 1.4 mm). 双熔敷极焊条电弧焊其电弧电压是由双焊芯之间间隙决定的，焊条压成后间隙已定，其焊接电弧电压在焊接过程中基本不变，这是由双熔敷极焊条电弧焊的工艺特性决定的[7]. 选用 Q235 钢作为试板母材，尺寸为 200 mm × 100 mm × 10 mm，试验前试件表面进行机械加工，防止铁锈、油污影响焊接质量.

试验采用平板堆焊方法，焊接速度为 330 mm/min. 焊后截取焊缝断面打磨抛光腐蚀后，用低倍光学显微镜拍摄焊接接头形貌，测量焊缝熔深. 试验首先采用四因素三水平 $L_9(3^4)$ 正交试验法确定频率(f)、峰值电流(I_p)、基值电流(I_b)和占空比(D)四个脉冲参数对熔深影响程度的大小. 在正交试验基础上，进而对 I_p，f，D，I_b 四因素分别优选固定三因素，试验研究第四因素水平的变化对熔深的影响规律.

综合正交试验和 I_p，f，D，I_b 四因素对熔深影响的规律，优选四个脉冲参数组合，并进行焊缝熔深试验测试.

3 试验结果及分析

3.1 脉冲参数的正交试验

四个脉冲参数，每个参数取三个不同水平的数值，组成 $L_9(3^4)$ 正交试验表，试验结果分析如表 1 所示. 表中 K_1，K_2 和 K_3 分别代表各列中对应水平位级所得熔深的代数和，而 k_1，k_2 和 k_3 则分别是 K_1，K_2 和 K_3 除以各水平重复次数(试验中为 3 次)所得平均值. R 为数据极差，即

$$R = \max\{k_1, k_2, k_3\} - \min\{k_1, k_2, k_3\}$$

数据极差代表了对应因素水平变动时对试验结果(熔深)影响的大小，极差越大表示该因素水平变动时对试验结果(熔深)的影响就越大.

从表 1 中可直观看出，在设计的九组试验中 3 号试验所得熔深最大，即脉冲参数组合为频率 3.5 Hz，峰值电流 230 A，基值电流 170 A，占空比 50%. 由极差 R 的分析可知，四因素对焊缝熔深影响程度不同，影响程度由大到小的次序为峰值电流→频率→占空比→基值电流. 表明试验过程中若想获得较大熔深特别要求控制好峰值电流，其次是频率和占空比，基值电流的影响相对较小.

表 1 脉冲参数正交试验结果分析表

Table 1 Results of orthogonal experiment with pulsed parameters

试验编号	频率 f/Hz	峰值电流 I_p/A	基值电流 I_b/A	占空比 D(%)	指标熔深 H/mm
1	3.5	200	150	30	1.51
2	3.5	215	160	40	1.32
3	3.5	230	170	50	2.21
4	4.5	200	160	50	1.43
5	4.5	215	170	30	0.74
6	4.5	230	150	40	1.5
7	5.5	200	170	40	1.33
8	5.5	215	150	50	1.31
9	5.5	230	160	30	1.75
K_1	5.04	4.27	4.32	4.00	—
K_2	3.67	3.37	4.50	4.15	—
K_3	4.39	5.46	4.28	4.95	—
k_1	1.680	1.423	1.440	1.333	—
k_2	1.223	1.123	1.500	1.383	—
k_3	1.463	1.820	1.427	1.650	—
R	0.457	0.697	0.073	0.317	—

3.2 脉冲参数对熔深大小的影响规律

3.2.1 峰值电流对熔深的影响

脉冲电源的焊接电流有峰值电流 I_p 和基值电流 I_b 两部分，焊接过程中电流变化由示波器测定如图 2 所示，电流值的改变会直接影响到焊缝熔深的大小. 图 3 显示熔深随峰值电流的变化趋势. 其它参数频率 f 为 3.5 Hz，基值电流 I_b 为 160 A，占空比 D 为 50%. 在试验范围内，随着峰值电流的增加，热输入加大，母材熔化量增多，焊缝熔深增加明显，表现为曲线较陡，说明随着峰值电流的增加熔深的增加速度加快，当 I_p 达到230 ~ 240 A时，熔深呈缓降

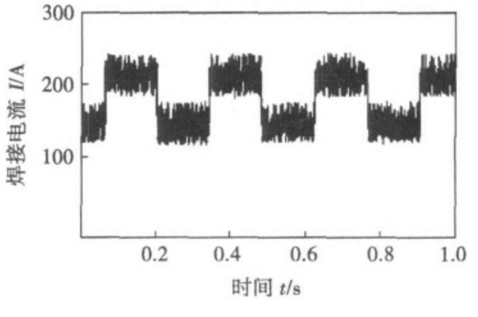

图 2 焊接电流波形(I_p = 230 A，f = 3.5 Hz，D = 50%，I_b = 160 A)

Fig. 2 Waveform of welding current (I_p = 230 A, f = 3.5 Hz, D = 50%, I_b = 160 A)

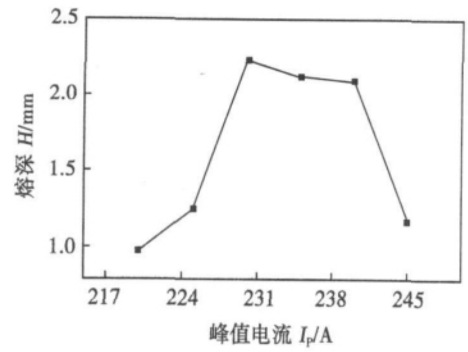

图 3　峰值电流对熔深的影响

Fig. 3　Effect of different peak current on weld penetration

趋势，但都在 2 mm 以上; 随着峰值电流进一步增大，焊条熔化增多，焊缝熔宽增加，焊接过程中电弧变得不稳定，飞溅量较大，熔深明显下降. 上述试验表明峰值电流 I_p 在 230 A 左右熔深较深.

3.2.2　频率对熔深的影响

频率代表着单位时间(s) 内的脉冲数目. 熔深随频率的变化如图 4 所示. 其它参数峰值电流 I_p 为 230 A，基值电流 I_b 为 160 A，占空比 D 为 50%. 随着频率的增加，焊接电流在峰值与基值之间的转化加快，焊接过程中电弧形态发生明显的变化，可观察到焊接电弧变得更加明亮，母材熔化量增多，表现为熔深缓慢增加，当频率增加为 3.5 Hz 时，熔深达到最大值; 频率进一步增加时，焊接过程中电弧的跳动变得剧烈，使得焊接热输入降低，焊缝熔深减小. 获得相对较大的熔深时，焊接脉冲频率在 3.3 ~ 3.7 Hz 之间.

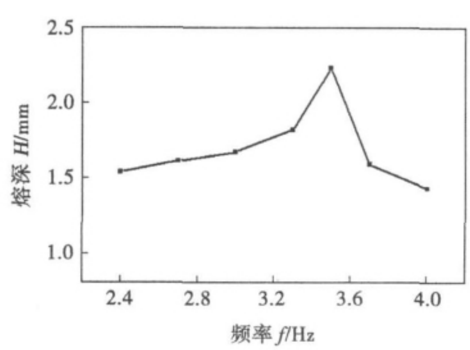

图 4　频率对熔深的影响

Fig. 4　Effect of different frequency on weld penetration

3.2.3　占空比对熔深的影响

占空比是指一个周期内峰值电流时间所占的百分比. 图 5 为峰值电流为 230 A、基值电流为 160 A、频率 3.5 Hz 时熔深随占空比的变化趋势. 占空比增加时焊接过程脉冲电流能量增大，焊接热输入加大，母材熔化量多，电弧对熔池的冲击力加大使熔深增加; 在占空比达到 50% 时熔深达到最大值; 占空比继续增加时，一个周期内峰值电流持续时间占的比例增大，焊条熔化加快，较多的熔敷金属铺展在焊缝表面，加之焊接电弧脉冲现象的减弱，焊缝熔深逐渐减小. 由图 5 中看出，占空比选择在 48% ~52% 范围内可以获得相对较大的熔深.

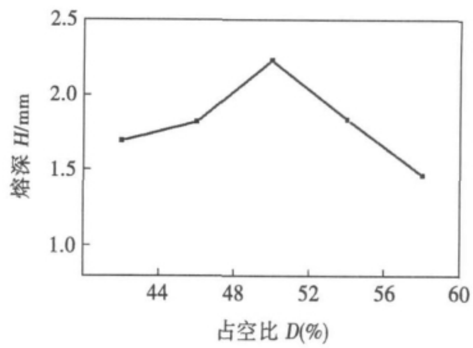

图 5　占空比对熔深的影响

Fig. 5　Effect of different duty ratio on weld penetration

3.2.4　基值电流对熔深的影响

图 6 为基值电流对焊缝熔深的影响趋势，峰值电流 I_p 为 230 A，频率 f 为 3.5 Hz，占空比 D 为 50%. 从图 6 中可以看出，熔深在基值电流 160 ~ 175 A 范围内缓降，但维持较大的数值(大于 2.0 mm) ; 当基值电流大于 175 A 时，基值电流继续增大，焊条受热熔化量增多，过多的熔化金属熔敷在母材表面，使得焊接电弧深入熔池内部受到制约，电弧的冲击力减弱，电弧对焊接熔池的搅动能力减小，从而使熔深减小. 基值电流是对熔深影响程度最小的一个脉冲参数. 在 160 ~ 175 A 范围内都可以获得相对较大熔深.

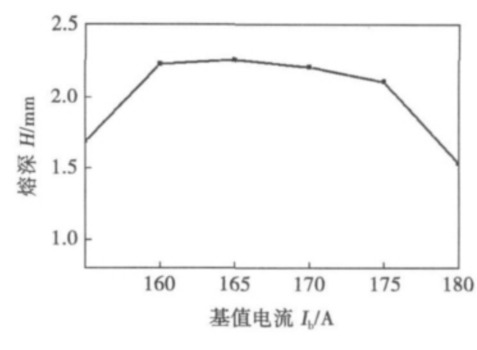

图 6　基值电流对熔深的影响

Fig. 6　Effect of different base current on weld penetration

3.3　优化脉冲参数组合试验

根据脉冲参数正交试验和 I_p，f，D，I_b 等对焊缝

熔深影响规律的试验研究,分别优选四个脉冲参数,即峰值电流为230 A,频率为3.5 Hz,占空比50%,基值电流160 A. 在其它工艺条件相同情况下,对优选组合状态进行表面堆焊,焊后焊缝横截面如图7a所示,焊缝获得较大的熔深,实测为2.23 mm.

用同一脉冲焊机,焊接电流选用195 A(相当于脉冲电源I_p =230 A,I_b =160 A),去掉脉冲(即I_p = I_b =195 A,脉冲频率f和占空比D调至最小值分别为0.2 Hz,1%),在其它焊接工艺参数相同的条件下进行表面堆焊,其焊后焊缝横截面如图7b所示,实测熔深为1.18 mm.

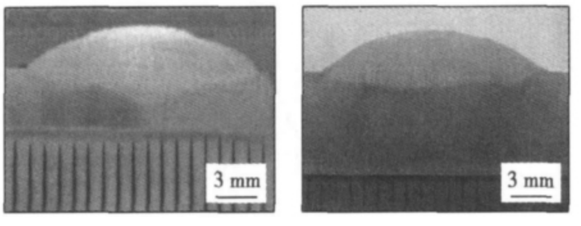

(a) 优选脉冲参数组合 (b) 无脉冲

图7 不同条件下的焊缝横截面

Fig. 7 Cross-section of weld under different condition

4 结 论

(1) 将脉冲电源应用于双熔敷极焊条电弧焊,脉冲参数对熔深的影响程度由大到小的次序为峰值电流、频率、占空比、基值电流.

(2) 脉冲参数的变化对焊缝熔深具有一定的影响,焊接过程中脉冲参数范围为峰值电流230~240 A,频率3.3~3.7 Hz,占空比48%~52%,基值电流160~175 A,焊后能够获得较大熔深.

(3) 脉冲电源应用于双熔敷极焊条电弧焊利于增加焊缝熔深. 脉冲频率、峰值电流、基值电流和占空比分别为3.5 Hz,230 A,160 A和50%是脉冲参数的优化组合,可获得较大熔深的焊缝. 为双熔敷极焊条电弧焊技术的应用提供新的电源.

参考文献:

[1] 姜焕中. 电弧焊及电渣焊[M]. 北京: 机械工业出版社, 1988.

[2] Erdal Karadeniz, Ugur Ozsara, Ceyhan Yildiz. The effect of process parameters on penetration in gas metal arc welding processes[J]. Materials & Design, 2007, 28(2): 649-656.

[3] 魏艳红, 徐艳利, 孙燕洁, 等. A-TIG焊接熔深增加机理[J]. 焊接学报, 2009, 30(2): 37-40.
Wei Yanhong, Xu Yanli, Sun Yanjie, *et al*. Mechanism of increasing welding penetration with A-TIG[J]. Transactions of the China Welding Institution, 2009, 30(2): 37-40.

[4] 秦国梁, 雷 振, 王旭友, 等. Nd: YAG激光+脉冲MAG电弧复合热源焊接参数对焊缝熔深的影响[J]. 机械工程学报, 2007, 43(1): 225-228.
Qin Guoliang, Lei Zhen, Wang Xuyou, *et al*. Influences of Nd: YAG laser + pulsed MAG arc hybrid welding parameters on weld penetration[J]. Chinese Journal of Mechanical Engineering, 2007, 43(1): 225-228.

[5] 李 桓, 郭 胜, 陈埒涛, 等. 脉冲埋弧焊工艺研究及焊缝熔深特征[J]. 焊接, 2004(7): 10-12, 23.
Li Huan, Guo Sheng, Chen Lietao, *et al*. Study on techniques and penetration characteristics of pulsed submerged arc welding[J]. Welding & Joining, 2004(7): 10-12, 23.

[6] 邹增大, 韩 彬, 曲士尧, 等. 双电极焊条单弧焊的电弧特性[J]. 焊接学报, 2004, 25(1): 5-7, 12.
Zou Zengda, Han Bin, Qu Shiyao, *et al*. Investigation on arc characteristic of twin electrode single arc welding[J]. Transactions of the China Welding Institution, 2004, 25(1): 5-7, 12.

[7] 邹增大, 韩 彬, 曲士尧, 等. 双电极焊条单弧焊工艺[J]. 焊接学报, 2004, 25(2): 15-18.
Zou Zengda, Han Bin, Qu Shiyao, *et al*. Twin electrode single arc technology[J]. Transactions of the China Welding Institution, 2004, 25(2): 15-18.

作者简介: 菅明健,男,1985年出生,硕士研究生. 研究方向为新材料及连接技术. Email: jianmingjian2005@yahoo.com.cn

通讯作者: 邹增大,男,教授. Email: zengdaz@sdu.edu.cn

mechanical mixture of TC1 base metal and LF6 base metal.

Key words: dissimilar matals of Ti/Al; friction stir welding; lap joint; microstrcture; element distribution

Comparision of corrosion properties for 5083 aluminum alloy friction stir welding and metal inert-gas welding weld

ZHAO Yadong[1], WANG Zhigang[1], SHEN Changbin[2], GE Jiping[2], Huang Zhenhui[3] (1. School of Mechanical Engineering, Anyang Institute of Technology, Anyang 455000, China; 2. School of Materials Science and Engineering, Dalian Jiaotong University, Dalian 116028, China; 3. R&D Center, CNR Tangshan Railway Vehicle Co., Ltd, Tangshan 063035, China). p 77 – 80

Abstract: The microstructures and corrosion properties of 5083 aluminum alloy friction stir welding (FSW) and MIG (metal inert-gas) weld were analyzed. The results showed that the FSW weld was characterized by its much finer grains, contrasting with the grains of MIG weld. Electrochemical corrosion test demonstrated that the corrosion potential of the FSW weld at the rotation rate of 300 r/min, and the traverse speed of 160 mm/min with 3°tool tilt was more positive than that of the MIG weld, meanwhile, the corrosion rate and the corrosion current density were less than those of the MIG weld, Rp (polarization resistance) of the FSW weld was larger than that of the MIG weld. The corrosion morphologies analysis showed that few shallow pits presented on the surface of the dissimilar weld. However, a large number of deeper pits emerged on the surfaces of two parent materials.

Key words: 5083 aluminum alloy; friction stir welding (FSW); metal inert-gas welding (MIG); weld; corrosion properties

Microstrucutre analysis of superplastic deformation on laser butt weld Ti-6Al-4V joint

CHENG Donghai, CHEN Yiping, HU Dean, WEI Qiang (School of Aeronautical Manufacturing Engineering, Nanchang Hangkong University, Nanchang 330063, China). p 81 – 84

Abstract: Microstructures of welded joints before and after superplastic deformation were observed by optical microscope, and the forming mechanism was discussed. The results indicated that increasing temperature and decreasing velocity were good for superplastic deformation, and the grains of base metal grew coarser and the phase ratio increased. Needle-like martensite phase of weld bead became shorter and wider, exhibiting globing trend under higher temperature. The maximal microhardness of cross section of weld bead after deformation is 380 HV, about 50 HV lower compares with original weld bead, which meets the requirnement of the actucal lead.

Key words: titanium alloy; welding/superplastic deformation; mirostructure

Microstructure and mechanical property of dissimilar material resistance spot welded joint of steel and aluminum alloy with electrode plate

ZHANG Weihua[1], SUN Daqian[1], LI Zhidong[2], LIU Dongyang[1], LI Dandan[1] (1. Key Laboratory of Automobile Materials, School of Materials Science and Engineering, Jilin University, Changchun 130022, China; 2. Engineering Training Center, Jilin University, Changchun 130022, China). p 85 – 88

Abstract: Dissimilar materials of H220YD high strength steel and 6008-T66 aluminum alloy had been joined by resistance spot welding with electrode plate. Microstructure and mechanical property of the dissimilar material welded joint were investigated. The results indicated that the welded joint was achieved by means of wetting and spreading of liquid aluminum alloy on solid steel surface, hence it could be regarded as a special welded-brazed joint. A thin dual-layered intermetallic compound layer composed of Fe_2Al_5 and $FeAl_3$ was formed on the steel/aluminum alloy interface. The diameter of aluminum alloy nugget of the welded joint reached the maximum value of 9.5 mm at welding speed of 14 kA and welding time of 300 ms. With the increase of welding current (8-14 kA), the tensile-shear load of the welded joint increased rapidly first (8-12 kA) and then became calm gradually (12-14 kA). The tensile-shear load was up to 4.3 kN at welding current of 12 kA and welding time of 300 ms, which was about 30% higher than that of the welded joint obtained without electrode plate. During tensile shear testing, the cracking developed through the brittle intermetallic compound layer and partially in the aluminum alloy nugget.

Key words: high strength steel; aluminum alloy; resistance spot welding; electrode plate

Investigation on penetration of pulsed twin deposition electrode arc welding

JIAN Mingjian, ZOU Zengda, WANG Yufu (Key Laboratory for Liquid-Solid Structural Evolution & Processing of Materials Ministry of Education, Shandong University, Jinan 250061, China). p 89 – 92

Abstract: Effects of pulsed parameters on weld penetration with the method of orthogonal experiment were researched when pulse power supply was applied to twin deposition electrode arc welding. Results of orthogonal experiment indicated the change of pulsed parameters could result in the corresponding change of weld penetration, and the descending order of pulsed parameters influencing weld penetration was as follows: peak current > frequency > duty ratio > base current. Greater penetration could be obtained with these pulsed parameters: peak current of 230-240 A, frequency of 3.3-3.7 Hz, duty ratio of 48%-52% and base current of 160-175 A. Optimal combination of pulse parameters of obtaining greater penetration is determined, which is frequency of 3.5 Hz, peak current of 230 A, base current of 160 A and duty ratio of 50%. Weld penetration increases when pulse power supply is applied to twin deposition electrode arc welding.

Key words: pulsed parameters; orthogonal experiment; weld penetration

Effect of processing parameters on microstructure and mechanical properties of pure copper joints made by friction stir welding

LI Xiawei, ZHANG Datong, QIU Cheng, ZHANG Wen (State Engineering Research Center for Metallic Materials Net-shape Processing, South China University of Technology, Guangzhou 510640, China). p 93 – 96

Abstract: The main objective of this investigation was to apply friction stir welding (FSW) for joining of pure copper plate which is 3 mm thick. Defect free welds were obtained at a constant rotation speed of 800 r/min and travel speed ranging from 60 mm/min to 300 mm/min. The influence of welding parameters on the microstructure and mechanical properties of the pure copper joints were investigated. The joints exhibit four distinct zones, parent material, heat affect zone, thermo-mechanically